Radiation Measurements 97 (2017) 20–27

Contents lists available at ScienceDirect

Radiation Measurements

journal homepage: www.elsevier.com/locate/radmeas

Thermoluminescence glow curves in preheated feldspar samples: An interpretation based on random defect distributions

George S. Polymeris [a, *], Vasilis Pagonis [b], George Kitis [c]

[a] Institute of Nuclear Sciences, Ankara University, 06100 Beşevler, Ankara, Turkey
[b] Physics Department, McDaniel College, Westminster, MD 21157, USA
[c] Nuclear Physics Laboratory, Aristotle University of Thessaloniki, 54124 Thessaloniki, Greece

HIGHLIGHTS

- TL glow curves for four types of preheated feldspar samples were measured.
- The experimental data is analyzed using two different methods within a model of localized electronic recombination.
- The model deals with random distribution of donor-acceptor pairs, with nearest-neighbor interaction.
- Low temperature TL signal for preheat below 260 °C is consistent with the presence of a continuous distribution of energies.
- A single trap characterized by a single activation energy E = (1.20 ± 0.09) eV at temperatures higher than 300 °C.

ARTICLE INFO

Article history:
Received 25 October 2016
Received in revised form
13 December 2016
Accepted 26 December 2016
Available online 28 December 2016

Keywords:
Thermoluminescence in feldspars
Kinetic analysis
Feldspar glow curves
Random defect distribution

ABSTRACT

Thermoluminescence (TL) glow curves from feldspar samples have been studied extensively in luminescence dating and dosimetry applications. However, the mechanism responsible for their unusual shape and behavior in preheated samples is not well understood. This paper presents new experimental TL glow curves for four types of preheated feldspar samples; an orthoclase, a sanidine and two microclines. Both the preheat temperature and the duration of the preheat are varied, before measurement of the remnant TL glow curve. Kinetic analysis of the experimental results is carried out using a recently proposed physical kinetic model which describes localized electronic recombination in a random distribution of donor-acceptor pairs, with nearest-neighbor interaction. The experimental data are analyzed using two different methods within the model. In the first method one follows the development of the distribution of nearest neighbor distances for each of the four stages of the experiment, namely irradiation followed by heating to a temperature and holding the sample at this temperature for certain time, and finally measurement of the TL glow curve. In the second method the TL glow curves are analyzed by using a single adjustable parameter in the model, which characterizes the thermal history of the sample. Good agreement is found between the two methods. However, the second method is much simpler to use in practical situations, and in principle it can be applied for any thermally or optically pretreated feldspar sample.

1. Introduction

The kinetics of thermoluminescence (TL) signals from feldspars have been studied extensively during the past 30 years, due to their importance in luminescence dosimetry and dating applications (see for example the books by Bøtter-Jensen et al., 2003; Chen and Pagonis, 2011). These studies have established that the main luminescence mechanism in feldspars is quantum mechanical tunneling (Wintle, 1977; Visocekas et al., 1996), and that it can be characterized by two types of trap depth, an optical trap depth estimated to be ~2–2.5 eV, and a thermal trap depth estimated to be in the range 1.6–1.8 eV with some estimates at ~2 eV (Clark and Sanderson, 1994; Duller, 1995; Chruścińska, 2001; Chruścińska et al., 2001; Murray et al., 2009; Poolton et al., 2009; Jain and Ankjærgaard, 2011; Li and Li, 2013; Kars et al., 2013).

From a modeling point of view, the model developed by Jain

* Corresponding author.
E-mail address: gspolymeris@ankara.edu.tr (G.S. Polymeris).

http://dx.doi.org/10.1016/j.radmeas.2016.12.012
1350-4487/

et al. (2012) has been a major development in this research area, and has contributed in the understanding of tunneling phenomena in a random distribution of electron-hole pairs. Kitis and Pagonis (2013) quantified the semi-analytical model of Jain et al. (2012) by deriving exact analytical expressions for different experimental stimulation modes. Pagonis et al. (2013) obtained approximate expressions for the time development of nearest neighbor distribution during various types of luminescence experiments. The analytical equations by Kitis and Pagonis (2013) have now been used to describe luminescence signals from a variety of feldspars and apatites (Polymeris et al., 2013; Şahiner et al., 2014; Sfampa et al., 2015; Kitis et al., 2016).

In regards to TL glow curves in feldspars, despite extensive experimental and modeling work in the past few years, the exact underlying mechanism is still an open research question. A detailed description of previous efforts to analyze TL glow curves in feldspars was given recently by Pagonis et al. (2014). These authors studied TL glow curves in a plagioclase feldspar using the T_{max}–T_{stop} and initial rise technique of glow curve analysis. Application of these method of analysis showed the presence of a continuous distribution of energy levels for samples preheated up to ~260 °C, with energies between 0.8 and 1.5 eV. By contrast, when the same samples were preheated at higher temperatures above 300 °C, it was found that the thermal activation energy was practically constant with a value of E~1.4–1.6 eV. This study suggested that the TL glow curves in feldspars can be described by the presence of a continuum of energies in the range 0.8–1.2 eV, combined with a single trap with an energy E~1.5 eV. This conclusion is consistent with extensive time-resolved and OSL/TL studies in feldspars (Jain and Ankjærgaard, 2011; Morthekai et al., 2012; Pagonis et al., 2012, 2014; Kars et al., 2013).

The overall purpose of this paper is to provide a quantitative description of a series of TL glow curves obtained for feldspars which underwent high temperature preheating above 300 °C.

The specific goals of the paper are:

(a) To investigate the nature of the traps responsible for the TL glow curves, and specifically whether the experimental data supports a continuous distribution of energy levels, or a single energy level, or both.
(b) To carry out a detailed quantitative analysis of a series of TL glow curves obtained by thermally bleaching the TL signal at different preheating times, and at a fixed temperature of 300 °C.
(c) To repeat this kinetic analysis using the *same* kinetic parameters as in (b), for different samples which were preheated at several temperatures, while keeping the preheat time fixed.
(d) To compare the results of the kinetic analysis from different feldspar samples.
(e) To develop a new simpler method for analyzing a series of TL glow curves measured in preheated feldspar samples.

2. Experimental

The luminescence signals from the feldspar samples used in this paper have been studied previously in Polymeris et al. (2013). These authors investigated the possibility of using thermoluminescence (TL) for structural characterization of ten K-feldspar samples. They found a good correlation between TL sensitivity and individual K-feldspar structure and suggested that these samples are ideal for investigating basic TL, OSL and IRSL signals. The group of samples studied by these authors consisted of 3 sanidine, 4 orthoclase and 3 microcline feldspars.

The experimental setup, sample preparation and experimental conditions for the present paper were described previously in Polymeris et al. (2013), and will not be repeated here. Four of the samples studied previously in Polymeris et al. (2013) are used in this paper, namely microcline samples KST4 and ELD1, sanidine sample SAM3, and orthoclase sample VRS3 (see Polymeris et al., 2013, their Table 1).

The first experimental protocol used in this paper was as follows. An irradiated aliquot of the material is heated to a fixed preheat temperature of 300 °C for a variable preheating time t_{PH}, followed by measurement of its TL signal. The specific steps in the protocol are:

1. Test dose 40 Gy.
2. Preheat at temperature $T_{PH} = 300^oC$ and for a preheat time $t_{PH} = 0,1,3,5,10,17,25,37,50,75$ s.
3. Measurement of TL signal by heating up to 500 °C with a linear heating rate $\beta = 1$ K/s.
4. Repeat steps 1–3 for a new preheat time t_{PH}.

In the second experimental protocol, the same irradiated sample was preheated to T_{PH} ranging between 125 °C and 350 °C and for a fixed preheating time $t_{PH} = 10s$, followed by measurement of its TL signal. The purpose of this second set of experiments is to investigate whether the *same* kinetic parameters in the model can describe the TL glow curves measured with either a variable preheat time, or with a variable preheat temperature. Both the conditions of TL measurements and the irradiation dose are same as presented above.

These two experimental protocols were applied using a single aliquot, and this makes it necessary to test for sensitivity changes which may occur during repeated heating and irradiation. The sensitivity test was performed by measuring the TL signals before and after the end of the protocols. As in the previous studies by Polymeris et al. (2013), it was found that the sensitivity of all samples showed excellent stability, and that the reproducibility of the signals was better that 2%. It was concluded that there was no need for applying sensitivity corrections in these experiments.

3. General characteristics of the TL glow curves-the initial rise method

Fig. 1 shows the TL glow curves for all four samples, measured using the second protocol with a fixed preheat time of 10 s for a variable preheating temperature T_{PH}, followed by measurement of the TL signal. Fig. 2 shows the TL glow curves for all four samples, measured using the first protocol with a fixed preheat temperature of 300 °C and for a variable preheating time t_{PH}, followed by measurement of the TL signal. There are clear inflection points indicated by the arrows in Fig. 1a and b, supporting the idea that the TL signal is due to multiple energy levels.

In both Figs. 1 and 2, the TL glow curves shift towards higher temperatures as either the preheat time or the preheat temperature are increased. However, in all these sets of TL glow curves one observes that the high temperature side of the TL glow curves remains unaffected, while the lower temperature side gradually gets reduced. This observation is consistent with the tunneling model of Jain et al. (2012), which describes the TL signals within the framework of a random distribution of door-acceptor pairs, and with nearest neighbor interaction. As one increases either the preheat time or the preheat temperature, one expects that nearby

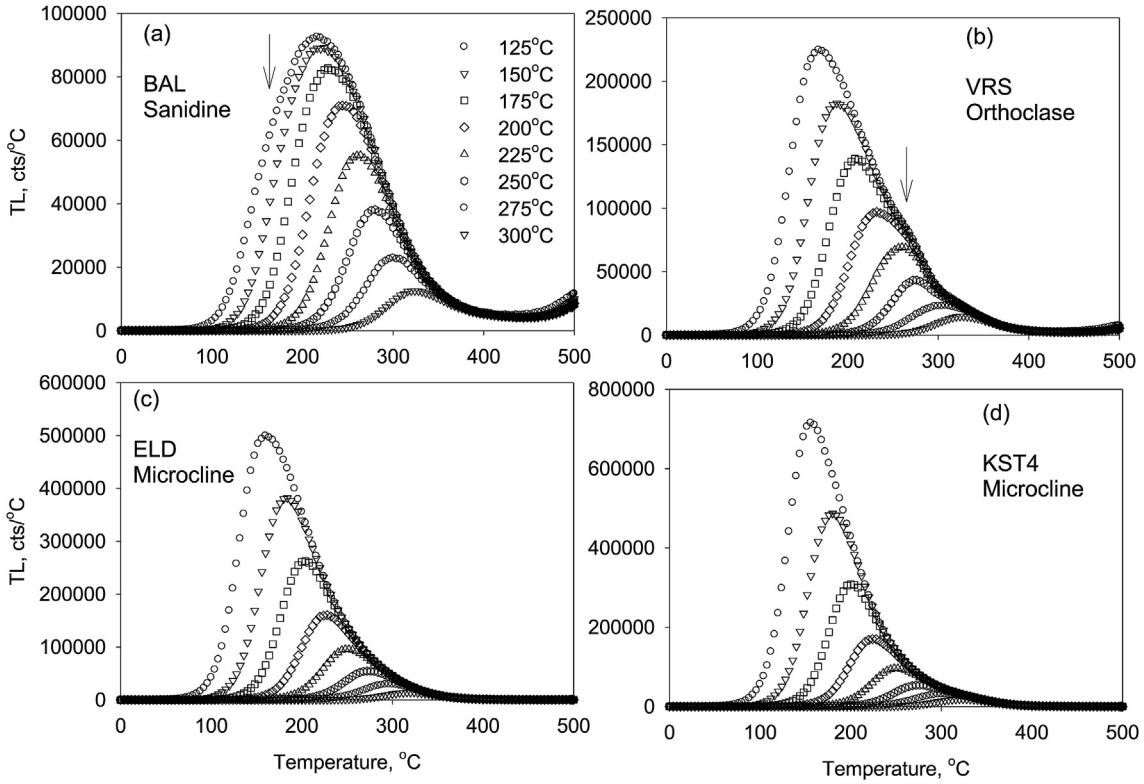

Fig. 1. TL glow curves measured in the second experimental protocol for four feldspar samples, with a fixed preheat time t = 10 s at variable preheat temperatures between 125 °C and 350 °C, in steps of 25 °C.

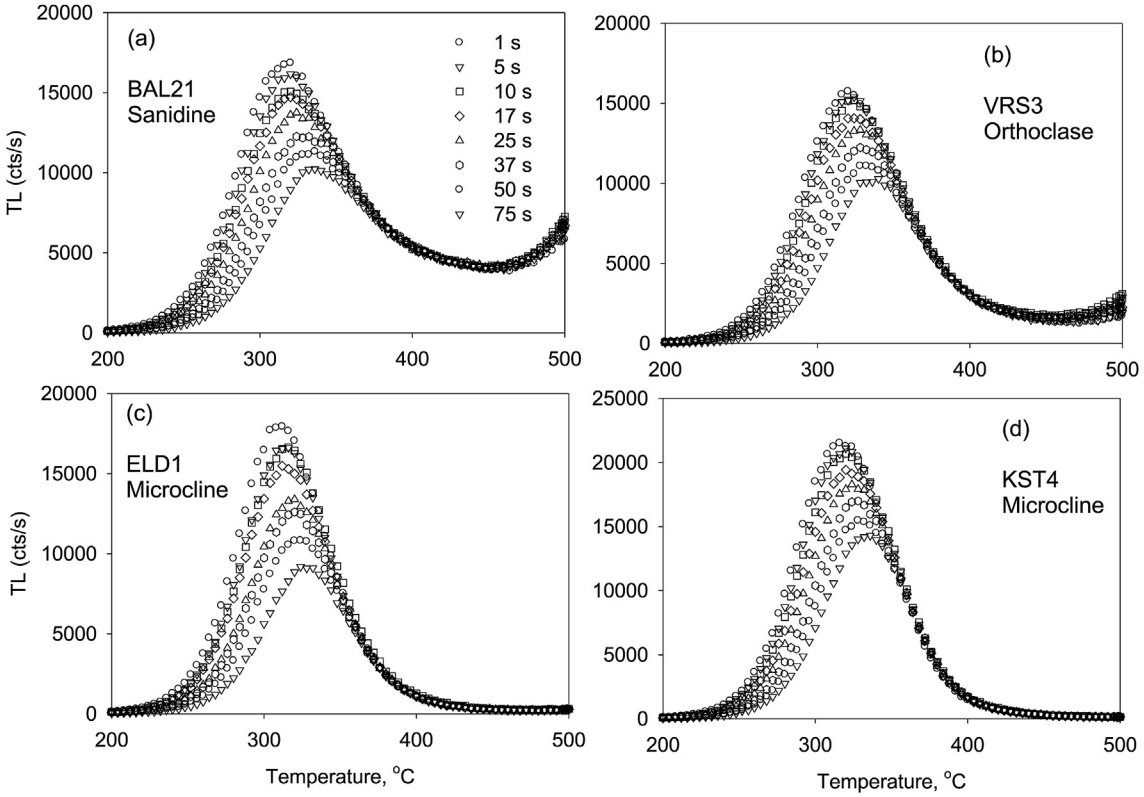

Fig. 2. TL glow curves measured in the first experimental protocol for the same four feldspar samples as in Fig. 1, with a variable preheat time t = 0–75 s, at a fixed preheat temperature 300 °C.

donor-acceptor pairs will recombine first, while more distant pairs will remain unaffected. This in turn will lead to a reduction of the luminescence signal in the low temperature side of the TL glow curves, since it is reasonable to assume that this part of the TL glow curve corresponds to shorter pair distances. This effect of thermal or optical stimulation on the low temperature side of the TL glow curves was previously demonstrated by Jain et al. (2012, their Fig. 9) who showed that the high temperature side of the TL glow curve remains unaffected.

Fig. 3a and b shows the results of applying the well-known initial rise method of analysis to the TL glow curves in Figs. 1 and 2, correspondingly. Fig. 3a shows that samples preheated at low temperatures below 260 °C show a remarkably consistent set of gradually increasing E-values from 0.8 eV up to 1.2 eV, for all four samples. These results are consistent with the analysis carried out in a microcline sample by Pagonis et al. (2014), who found a continuous distribution of energies in the same temperature and energy range. By contrast, Fig. 3b shows that for samples preheated above 300 °C one observes an almost constant value of the activation energy, with an average of E=(1.30 ± 0.09) eV obtained for all preheat times and all four samples. This again is consistent with the experimental results by Pagonis et al. (2014).

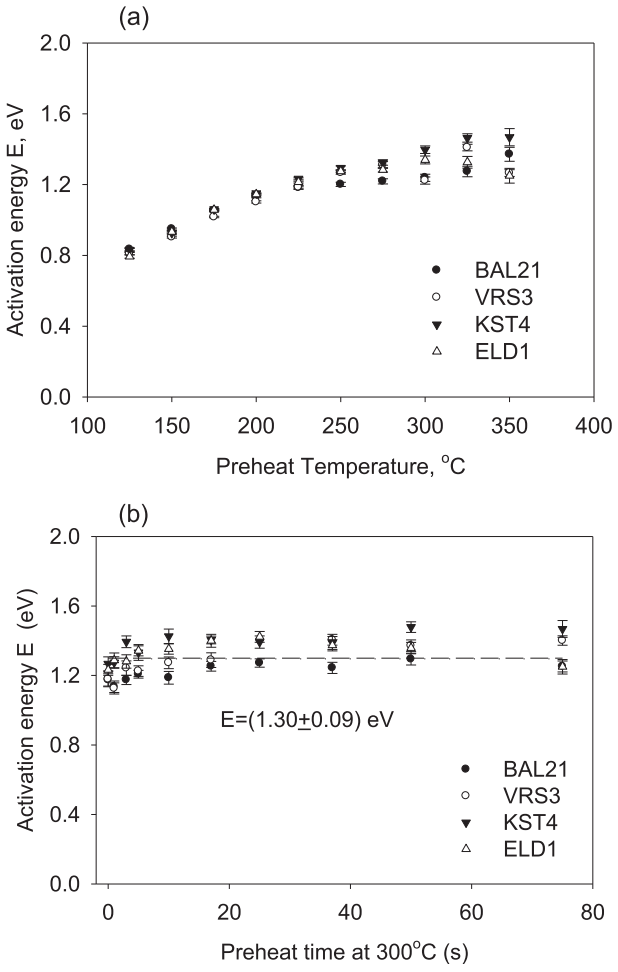

Fig. 3. (a) The initial rise method of analysis is applied to the experimental data in Fig. 1. A continuous increase of the activation energy E is seen for preheat temperatures below 260 °C for all 4 feldspar samples. This supports the presence of a continuous distribution of thermal activation energies between 0.8 and 1.2 eV. A single value of E is observed for preheat temperatures above ~260 °C, within experimental error. (b) The initial rise method applied to the data in Fig. 2. A single value of E is observed for all preheat times within statistical error, supporting the presence of a single trap with an average thermal activation energy E=(1.30 ± 0.09) eV.

4. The model: effect of preheating on TL glow curves

There are three versions of the model by Jain et al. (2012) in the literature. These three versions of the model were recently summarized by Kitis and Pagonis (2013), and will not be repeated here. The analysis of the TL glow curves in this paper is based on the version proposed by Pagonis et al. (2013), and this version of the model has been shown to produce the same results as the exact system of differential equations in the original model by Jain et al. (2012). These authors showed that the concentration of charge carriers during optical or thermal stimulation in the model is given by:

$$n(r',t) = n_0 3(r')^2 \exp\left[-(r')^3\right] \exp\left[-\exp\left(-(\rho')^{-1/3} r'\right) \int_0^t A dt'\right] \quad (1)$$

where A represents the probability of thermal/optical stimulation, n_o is the total initial number of donors and ρ' is the constant dimensionless density of acceptors in the system. Equation (1) describes the evolution of the distribution of electrons $n(r',t)$ in the ground state as a function of two parameters, namely the time t elapsed since the beginning of the optical or thermal stimulation, and the dimensionless distance parameter r'. This equation is valid for several types of excitation used in typical TL or OSL experiments, and the integral in equation (1) can be evaluated for the different experimental excitation modes.

In order to simulate accurately the effect of preheating on a TL glow curve, one needs to include the detailed experimental procedure which involves the following distinct stages:

Step 1: Irradiation stage.
Step 2: Sample is heated up to a preheat temperature T_{PH} with a linear heating rate.
Step 3: After the sample reaches the preheat temperature T_{PH}, it is kept there for a preheat time t_{PH}. This is the isothermal part of the experiment.
Step 4: The sample is heated from room temperature up to 500 °C with a linear heating rate $\beta = 1$ *K/s* in order to measure the remnant TL signal (R-TL).

The key point in the simulations is that the *final* distribution of remaining charge carriers $n(r',t)$ at the end of each step will act as the *initial* concentration of carriers for the next stage of this multiple step procedure. For example, the values of $n(r',t)$ at the end of stage 2 will be used as the initial values of $n(r',t)$ for stage 3, etc.

In *Step 1* it is assumed that a freshly irradiated sample is described by a full distribution of electron-hole pairs, described by the following symmetric probability distribution function $n(r',t=0)$ (Jain et al., 2012):

$$n(r',0) = 3n_0(r')^2 \exp\left[-(r')^3\right] \quad (2)$$

In *Step 2* the sample is heated up to the preheat temperature T_{PH} with a linear heating rate $\beta = 1K/s$. During this preheat stage the rate of thermal excitation is $A_{TL} = sexp(-E/kT)$, where the parameters s and E are the frequency factor and thermal activation energy of the trap correspondingly. The temperature $T(t)$ is increased linearly with a constant heating rate β according to $T(t) = T_o + \beta t$, with T_o representing the starting temperature in the heating process. During *Step 2*, the distribution of charge carriers is found by

substituting $A_{TL} = s\exp(-E/kT)$ in equation (1) to obtain:

$$n_{PH}(r',t) = n(r',0)\exp\left[-\exp\left(-(\rho')^{-1/3}r'\right)\int_0^t s\exp\left[-\frac{E}{k(T_o+\beta t')}\right]dt'\right] \quad (3)$$

where $n(r',0)$ is given by equation (2). The integral in equation (3) is the well-known exponential integral of TL theory, which can be approximated accurately by the first two terms of its series (see for example the book by Chen and Pagonis (2011), Chapter 15):

$$\int_0^T A dt' = \frac{skT^2}{\beta E}\exp\left(-\frac{E}{kT}\right)\left(1-\frac{2kT}{E}\right) \quad (4)$$

By substituting (4) into equation (3), and by setting $T = T_{PH}$, one obtains the concentration of remaining carriers at the end of *Step 2*:

$$n_{PH}(r',T_{PH}) = n(r',0)\exp\left[-\exp\left(-(\rho')^{-1/3}r'\right)\left\{\frac{skT_{PH}^2}{\beta E}e^{-\frac{E}{kT_{PH}}}\left(1-\frac{2kT_{PH}}{E}\right)\right\}\right] \quad (5)$$

After the sample reaches the preheat temperature T_{PH}, it is kept there for a preheat time t_{PH}. During this isothermal part of the experiment the rate of thermal excitation $A_{PH} = sexp(-E/kT_{PH})$ is constant and therefore the distribution of remaining electron-hole pairs at the end of *Stage 3* is:

$$n(r',t_{PH}) = n_{PH}(r',T_{PH})\exp\left[-\exp\left(-(\rho')^{-1/3}r'\right)s\exp(-E/kT_{PH})t_{PH}\right] \quad (6)$$

where $n(r', T_{PH})$ is given by equation (5).

During *Stage 4* of the experiment, the sample is heated again with a linear heating rate from room temperature up to 500 °C, in order to measure the remnant-TL signal. One can use again equation (1) with the probability of thermal excitation $A_{TL} = s\exp(-E/kT)$ and the temperature increases again linearly with time. The concentration of remaining carriers during this TL measurement is found from:

$$n(r',t) = n(r',t_{PH})\exp\left[-\exp\left(-(\rho')^{-1/3}r'\right)s\int_0^t \exp\left(-\frac{E}{k(T_o+\beta t')}\right)dt'\right] \quad (7)$$

where $n(r',t_{PH})$ is given by equation (6). By using once more the approximation of the exponential integral, the last equation becomes:

$$n(r',t) = n(r',t_{PH})\exp\left[-\exp\left(-(\rho')^{-1/3}r'\right)\times\left\{\frac{skT^2}{\beta E}e^{-\frac{E}{kT}}\left(1-\frac{2kT}{E}\right)\right\}\right] \quad (8)$$

Equation (8) (with the associated equations (2), (5) and (6)) is the desired analytical equation containing the experimental parameters t_{PH}, T_{PH}, β and the adjustable parameters ρ',E, s which characterize the physical properties of the sample.

By numerically integrating equation (8) over the dimensionless distance variable r', one finds the total number of electrons in the ground state at time t during the TL experiment:

$$n_{TL}(t) = \int_0^\infty n(r',t)\,dr' \quad (9)$$

The luminescence intensity $L_{R\text{-}TL}(t)$ of the R-TL signal is the time derivative of equation (9):

$$L_{R-TL}(t) = -\frac{dn_{TL}(t)}{dt} \quad (10)$$

Equations (2), (5), (6) and (8) are the analytical equations for evaluating the distribution $n(r',t)$ of electrons in the ground state of the system, at the different stages 1–4 of the simulation. Once $n(r',t)$ is calculated using equation (8), the TL intensity is calculated using numerical integration of equation (9) over the distance r', and by using numerical differentiation of equation (10) over the time variable t.

Fig. 4a shows the simulated distribution of distances $n(r',t)$ at the end of the different stages 1–4 of the simulation. The parameters used in this simulation are $t_{PH} = 10$ s, $T_{PH} = 300^oC$, $\beta = 1$ K/s, $\rho' = 0.013$, $E = 1.45$ eV, $s = 3.5 \times 10^{12}$ s^{-1}. Fig. 4a shows that the initially symmetric distribution of distances in the electron-hole pairs becomes gradually asymmetric, while overall it shifts towards larger distances. Physically this means that close by donor-acceptor pairs recombined first, and more distant pairs remain in the system at longer times.

Fig. 4b shows the simulated distribution of distances $n(r',t_{PH})$ at the beginning of stage 4, i.e. immediately before measurement of the TL glow curves, for a fixed preheat temperature of $T_{PH} = 300^oC$ and for variable preheating time $t_{PH} = 10,20,50$ s. The rest of the parameters in the model are identical to those in Fig. 4a.

Fig. 4c shows the simulated distribution of distances $n(r',t)$ at the beginning of stage 4, but for a variable preheat temperature of $T_{PH} = 300,325,350^oC$ and for a fixed preheating time $t_{PH} = 10$ s. The physical interpretation of Fig. 4b and c, is the same as for Fig. 4a: the distribution of distances of the electron-hole pairs shifts overall towards larger distances, since close by donor-acceptor pairs recombine first, followed by more distant pairs which are more stable over time.

5. Quantitative analysis of the TL glow curves

5.1. Analysis of the TL glow curves using equations (8)–(10)

We use the following procedure for fitting the series of TL glow curves obtained in the two protocols in this paper.

a. Use the initial rise method to obtain an estimate of the activation energy E, as in Fig. 3b.
b. By using the known experimental parameters t_{PH}, T_{PH}, β,E and an initial set of fitting parameters ρ', s in the model, use equations (8)–(10) to numerically evaluate the simulated TL glow curve. In practice the integration is carried out for range of the dimensionless distances $r' = 0–2$.
c. Adjust the parameters ρ',E, s in the model until a good fit is obtained in the model for the first curve in the set of experimental TL curves. The values of E should only be adjusted slightly, so that they remain consistent with the value of E from the initial rise method.

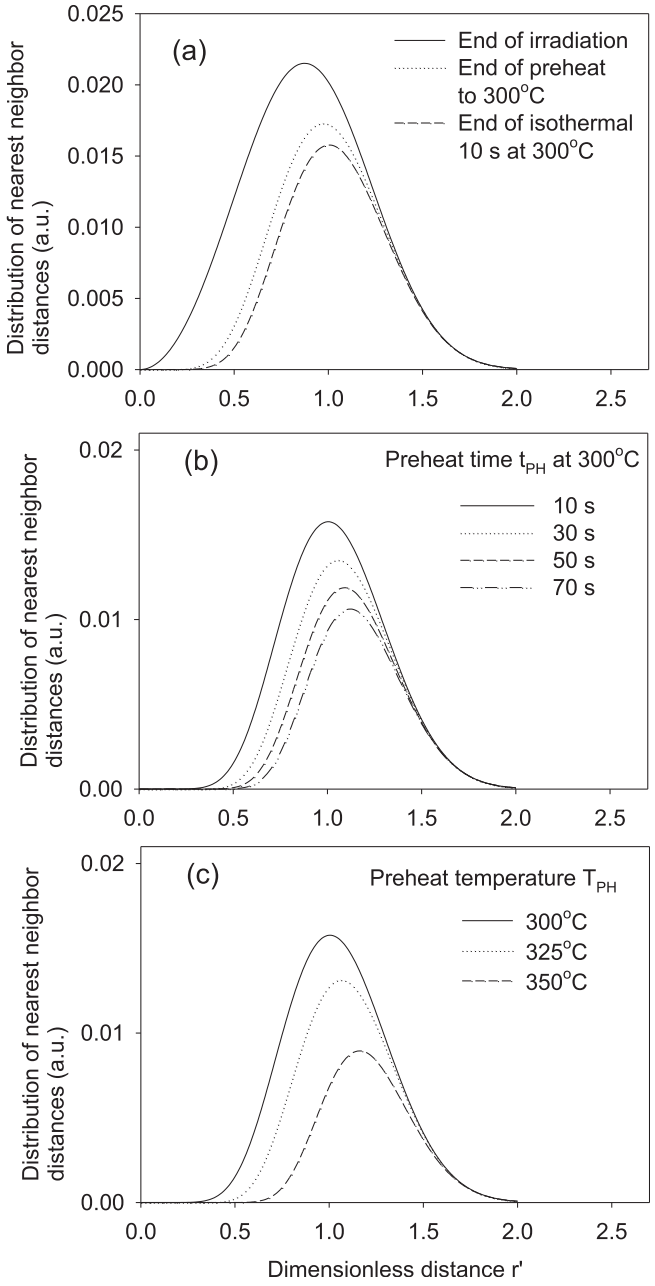

Fig. 4. Simulations of changes taking place in the nearest neighbor distribution $n(r',t)$ during measurement of the two experimental protocols in this paper.
(a) The distribution $n(r',t)$ at the end of each stage 1–3: irradiation, preheat up to preheat temperature T_{PH}, and isothermal decay at T_{PH} for a preheat time t_{PH}. The kinetic parameters used in the simulation are: $t_{PH} = 10$ s, $T_{PH} = 300°C$, $\beta = 1$ K/s, $\rho' = 0.013$, $E = 1.45$ eV, $s = 3.5 \times 10^{12}$ s^{-1}.
(b) The simulated distribution $n(r',t)$ just before measurement of the TL glow curves in the first experimental protocol, with a variable preheat time $t_{PH} = 1–75$ s and at a fixed preheat temperature $T_{PH} = 300°C$.
(c) The simulated $n(r',t)$ just before measuring the TL glow curves for the second experimental protocol, with variable preheat temperature $T_{PH} = 300$-$350°C$ at a fixed preheat time $t_{PH} = 10$ s.

d. Using the *same* parameters simulate a TL glow curve which is now compared with the second curve in the set.
e. Make minor adjustments to the parameters ρ', s, E in the model until a good fit is obtained for all curves in the experimental set of TL glow curves.

Fig. 5a shows the results of fitting the series of TL glow curves for microcline sample KST4, when using a fixed preheat temperature of 300 °C, and a variable preheating time $t_{PH} = 0–75$ s. The solid lines in Fig. 5a were obtained from the analytical equations (8)-(10) by using the procedure described above. The best fitting parameters for all the curves are $E = 1.45$ eV, $s = 3.5 \times 10^{12}$ s^{-1}, $\rho' = 0.015$.

Fig. 5b shows the experimental data for the second set of measurements for KST4, obtained for the same sample with a fixed preheat time $t_{PH} = 10$ s and a variable preheat temperature 300-350 °C. The *same* kinetic parameters are used in both simulations shown in Fig. 5a and b, although these describe a different type of experiment.

These results show that the series of experimental TL glow curves can be described accurately by considering the changing distributions $n(r',t)$ for each stage of the experimental procedure. Very good agreement is obtained between the model and the experimental data, and for both types of experiments described in this paper.

5.2. Analysis of the TL glow curves using a simplified method

Although the method used to fit the series of TL glow curves in Section 5.1 is exact and accurate, it is also somewhat tedious. We have therefore investigated the possibility of developing a faster fitting method within the same model as follows. We suggest that one can describe the changes taking place in $n(r',t)$ during stages 1–3 of the simulation by using a single dimensionless parameter α,

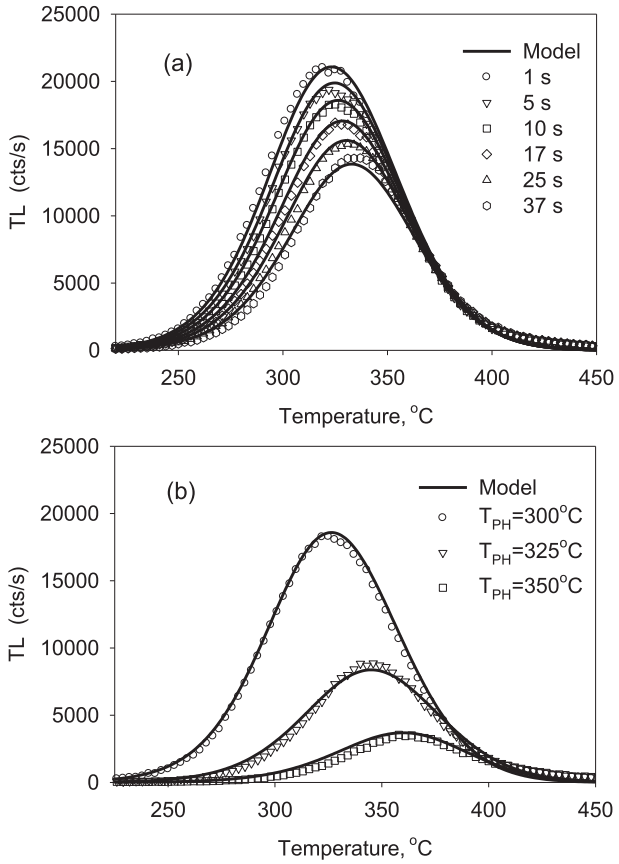

Fig. 5. Comparison of experimental data for microcline sample KST4 with the model described in the text. (a) TL glow curves measured with a variable preheat time $t_{PH} = 1–75$ s and at a fixed preheat temperature of $T_{PH} = 300°C$. (b) TL glow curves for a fixed preheat time $t_{PH} = 10$ s and a variable preheat temperature $T_{PH} = 300,325,350°C$. The same values of kinetic parameters are used for both sets of experimental data.

which is defined below. This dimensionless parameter encompasses the thermal history of the sample. By systematically varying this parameter α, one can describe a whole series of experimental TL glow curves similar to those shown in Figs. 1 and 2.

By combining the exponential terms in equations (2), (5), (6) and (8) we find:

$$n_{TL}(r',t) = n(r',0)\exp\Big[-\exp\Big(-(\rho')^{-1/3}r'\Big)\Big\{\alpha + \Big(skT^2\Big/\beta E\Big)\exp(-E/kT)(1-2kT/E)\Big\}\Big] \quad (11)$$

where

$$\alpha = \frac{skT_{PH}^2}{\beta E}e^{-\frac{E}{kT_{PH}}}\left(1-\frac{2kT_{PH}}{E}\right) + s_{thermal}e^{-E_{thermal}/kT_{PH}}t_{PH} \quad (12)$$

Clearly the dimensionless factor α is a functional that depends on the experimental parameters T_{PH}, t_{PH}, β and the kinetic parameters E,s of the sample.

In this type of simplified fitting procedure one proceeds as follows:

a. Use the initial rise method to obtain an estimate of the activation energy E
b. By using the known experimental parameters β, E and an initial set of fitting parameters ρ', s, α in the model, use equations (9) (10) and (11) to numerically evaluate the simulated TL glow curve.
c. Adjust the parameters ρ', E, s, α in the model until a good fit is obtained in the model for the first curve in the set of experimental TL curves. The values of E should only be adjusted slightly, to remain consistent with the E value from the initial rise method.
d. Using the *same* parameters and varying only α, simulate the rest of the series of TL glow curves in the set.

Fig. 6 shows the results of this simplified fitting procedure. The best fitting parameters for sample ELD1 and for the data in Fig. 6a are $E = 1.452$ eV, $s = 3.5 \times 10^{12}$ s^{-1}, $\rho' = 0.015$. As one may have expected, the fitting process was found to be rather sensitive to the values of the parameters E, s. The same parameters are used to fit the experimental data in Fig. 6b, with a slightly adjusted value of $s = 2 \times 10^{12}$. The best fitting values of the dimensionless factor α were α = 0,3,6.5,9, 13,22,30,42 for the data in Fig. 6a, and α = 0,25,120 for the data in Fig. 6b. Excellent agreement is found between the model and the whole series of TL glow curves for the microcline sample ELD1.

It is estimated that the accuracy of the parameters determined from the two methods presented in this paper is of the same order of magnitude. Specifically, the estimated accuracy in the E value from both methods is of the order of 0.01 eV, the accuracy for the frequency factor is within a multiplicative factor or 5, and the accuracy of the dimensionless density parameter is 0.001.

6. Discussion and conclusions

The method presented in Section 5.1 is completely general, and can be used for numerical evaluation of the TL glow curves for a sample which undergoes a complex series of either thermal or optical treatments. One simply has to follow the evolution of the functions $n(r',t)$ in each stage of the simulation, and set the final distribution of distances in each stage to be the initial distribution for the next stage. The method is exact, and in principle should be applicable for any combination of optical and/or thermal treatments.

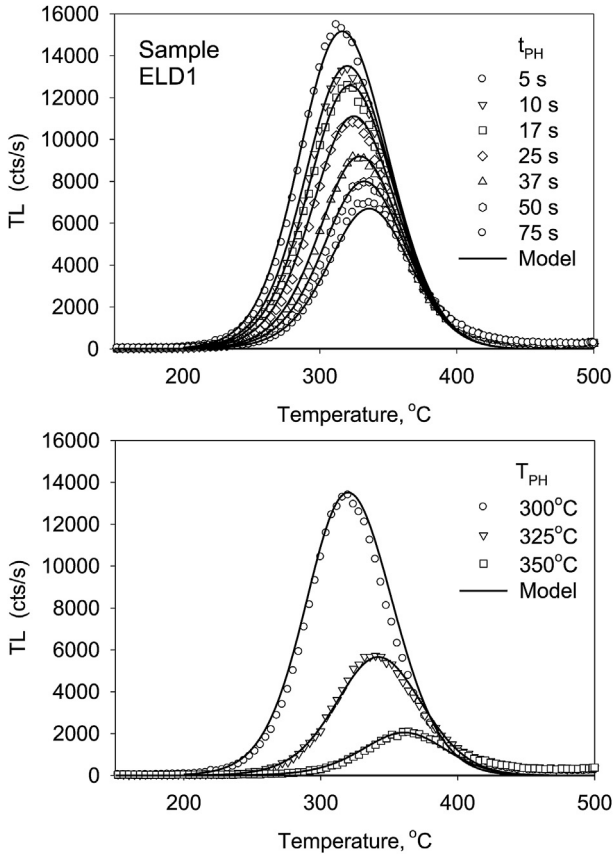

Fig. 6. Same type of analysis as in Fig. 5 for microcline sample ELD1, but using the simplified fitting approach described in the text. The same values of kinetic parameters are used for both sets of experimental data in (a) and (b).

However, the simpler method in Section 5.2 provides a much more efficient method of fitting a series of TL glow curves, again applicable for any type of pretreated sample. In this simpler method one describes the thermal/optical history of the samples by using the fitting parameter α, with an example given in equation (12).

The quantitative analysis of a series of TL glow curves in this paper is consistent with the following picture: the low temperature TL signal for irradiated samples preheated to low temperatures below 260 °C is consistent with the presence of a continuous distribution of energies between 0.8 and 1.2 eV. By contrast, the higher temperature TL signal for irradiated samples preheated to temperatures above 300 °C is consistent with the presence of a single trap characterized by a single activation energy E=(1.20 ± 0.09) eV. These experimental results are consistent with time-resolved experiments which supported the idea a single trap which is embedded in a continuum of energy states, possibly related to the band tail states in feldspars (Poolton et al., 2002; 2002b; 2009; Kars et al., 2013).

References

Bøtter-Jensen, L., McKeever, S.W.S., Wintle, A., 2003. Optically Stimulated Luminescence Dosimetry. Elsevier, Amsterdam.
Chen, R., Pagonis, V., 2011. Thermally and Optically Stimulated Luminescence: a Simulation Approach. Wiley and Sons, Chichester.
Chruścińska, A., 2001. The fractional glow technique as a tool of investigation of TL bleaching efficiency in K-feldspar. Geochronometria 20, 21–30.
Chruścińska, A., Oczokowski, H.L., Przegiętka, K.R., 2001. The parameters of traps in K-feldspars and the TL bleaching efficiency. Geochronometria 20, 15–20.
Clark, R.J., Sanderson, D.C.W., 1994. Photostimulated luminescence excitation

spectroscopy of feldspars and Micas. Radiat. Meas. 23, 641–646.
Duller, G.A.T., 1995. Infrared bleaching of the thermoluminescence of four feldspars. J. Phys. D. Appl. Phys. 28, 1244–1258.
Jain, M., Ankjærgaard, C., 2011. Towards a non-fading signal in feldspar: insight into charge transport and tunnelling from time-resolved optically stimulated luminescence. Radiat. Meas. 46, 292–309.
Jain, M., Guralnik, B., Andersen, M.T., 2012. Stimulated luminescence emission from localized recombination in randomly distributed defects. J. Phys. Condens. Matter 24, 385402.
Kars, R.H., Poolton, N.R.J., Jain, M., Ankjærgaard, C., Dorenbos, P., Wallinga, J., 2013. On the trap depth of the IR-sensitive trap in Na- and K-feldspar. Radiat. Meas. 59, 103–113.
Kitis, G., Polymeris, G.S., Sfampa, I.K., Prokic, M., Meriç, N., Pagonis, V., 2016. Prompt isothermal decay of thermoluminescence in MgB4O7:Dy, Na and LiB4O7:Cu, In dosimeters. Radiat. Meas. 84, 15–25.
Kitis, G., Pagonis, V., 2013. Analytical solutions for stimulated luminescence emission from tunneling recombination in random distributions of defects. J. Luminescence 137, 109–115.
Li, B., Li, S.-H., 2013. The effect of band-tail states on the thermal stability of the infrared stimulated luminescence from K-feldspar. J. Luminescence 136, 5–10.
Morthekai, P., Thomas, J., Padian, M.S., Balaram, V., Singhvi, A.K., 2012. Variable range hopping mechanism in band-tail states of feldspars: a time-resolved IRSL study. Radiat. Meas. 47, 857–863.
Murray, A.S., Buylaert, J.P., Thomsen, K.J., Jain, M., 2009. The effect of preheating on the IRSL signal from feldspar. Radiat. Meas. 44, 554–559.
Pagonis, V., Morthekai, P., Kitis, G., 2014. Kinetic analysis of thermoluminescence glow curves in feldspar: evidence of a continuous distribution of energies. Geochronometria 41 (2), 168–177.
Pagonis, V., Morthekai, P., Singhvi, A.K., Thomas, J., Balaram, V., Kitis, G., Chen, R., 2012. Time-resolved infrared stimulated luminescence signals in feldspars: analysis based on exponential and stretched exponential functions. J. Luminescence 132, 2330–2340.
Polymeris, G.S., Theodosoglou, E., Kitis, G., Tsirliganis, N.C., Koroneos, A., Paraskevopoulos, K.M., 2013. Preliminary results on structural state characterization of K-feldspars by using thermoluminescence. Mediter. Archaelogy Archaeom. 13, 155–161.
Poolton, N.R.J., Ozanyan, K.B., Wallinga, J., Murray, A.S., Botter-Jensen, L., 2002a. Electrons in feldspar II: a consideration of the influence of conduction band-tail states on luminescence processes. Phys. Chem. Miner. 29, 217–225.
Poolton, N.R.J., Wallinga, J., Murray, A.S., Bulur, E., Bøtter-Jensen, L., 2002b. Electrons in feldspar I: on the wave function of electrons trapped at simple lattice defects. Phys. Chem. Miner. 29, 210–216.
Poolton, N.R.J., Kars, R.H., Wallinga, J., Bos, A.J.J., 2009. Direct evidence for the participation of band-tails and excited-state tunnelling in the luminescence of irradiated feldspars. J. Physics-condensed Matter 21, 485505.
Şahiner, E., Meriç, N., Polymeris, G.S., 2014. Assessing the impact of IR stimulation at increasing temperatures to the OSL signal of contaminated quartz. Radiat. Meas. 68 (2014), 14–22.
Sfampa, I.K., Polymeris, G.S., Pagonis, V., Theodosoglou, E., Tsirliganis, N.C., Kitis, G., 2015. Correlation of basic TL, OSL and IRSL properties of ten K-feldspar samples of various origins. Nucl. Instrum. Methods Phys. Res. B 359, 89–98.
Visocekas, R., Tale, V., Zink, A., Spooner, N.A., Tale, I., 1996. Trap spectroscopy and TSL in feldspars. Radiat. Prot. Dosim. 66, 391–394.
Wintle, A.G., 1977. Detailed study of a thermoluminescent mineral exhibiting anomalous fading. J. Luminescence 15, 385–393.